

Triggered slip: observations of the 17 August 1999 Izmit (Turkey) earthquake using radar interferometry

Tim Wright, Eric Fielding¹, Barry Parsons

Department of Earth Sciences, University of Oxford, Parks Road, Oxford, UK.

Abstract. We use Synthetic Aperture Radar interferometry (InSAR) to map the displacement field of the 17 August 1999 Izmit earthquake, which largely conforms to that predicted for an elastic upper crust. We determine the earthquake source parameters and show that slip continues farther west than the mapped fault ruptures. We also show that additional sub-surface displacements occurred on parallel strands of the North Anatolian Fault Zone. We argue that this was caused by changes in static stress accompanying the mainshock, or by the dynamic release of regional stresses.

Introduction

The North Anatolian Fault Zone accommodates the westward motion of Turkey relative to Eurasia by right-lateral shear and regularly generates large earthquakes [Ambraseys, 1970; Barka, 1996] of which the Izmit earthquake was the largest in 60 years. The surface rupture (Fig. 1) was mapped for 100 km from Düzce in the east to the Gulf of Izmit. No rupture was observed on or west of the prominent Hersek delta (29.5° E) [Barka, 1999], but aftershocks continue for another 50 km beyond it. Estimates of future seismic hazard [Parsons *et al.*, 2000] in the Sea of Marmara depend crucially on the fault location and magnitude of slip in the Gulf of Izmit, because if little slip occurred west of Hersek, faults there were brought closer to failure.

Source parameters from InSAR

We have constructed interferograms using ERS1 and ERS2 35-day pairs spanning the earthquake (Fig. 2, Table 1a,b), as well as two other interferograms on adjacent tracks with longer temporal separations (Table 1c,d). The 35-day interferograms cover essentially the same interval and we would expect the range changes observed in both to be identical. There are, however, differences of ± 50 mm of range change, probably resulting from changing atmospheric conditions, with a possible small (less than 30 mm) contribution from orbital errors. The other interferograms are less coherent but provide valuable information about the lateral extent of faulting. In particular, the combination of descending interferogram *c* with ascending *a* or *b* gives measurements in two different look directions, and hence two components of the displacement vector at the western end of the rupture.

¹Also at Jet Propulsion Lab, Caltech, USA.

Copyright 2001 by the American Geophysical Union.

Paper number 2000GL011776.
0094-8276/01/2000GL011776\$05.00

Procedures for determining earthquake source parameters from radar interferometric data are well established [Massonnet and Feigl, 1998; Bürgmann *et al.*, 2000]. We use a hybrid Monte-Carlo, downhill simplex inversion procedure [Wright *et al.*, 1999] to determine best-fitting model parameters. This procedure minimises the misfit between our interferometric measurements of range change, sampled at discrete locations, and those predicted by an elastic dislocation model [Okada, 1985] of the earthquake. We fix the fault plane location to coincide with the surface rupture on-shore, solving for the offshore location. We aim to fit the data with as simple a model as possible, because the reduction in misfit obtained from more complex models is small. We perform the inversion procedure twice, first using interferograms *a, c, d* and a second time using *b, c, d*. The difference between the two inversion results gives us an indication of the errors in our model parameters (Table 2) resulting from atmospheric and orbital effects: slip magnitudes agree to within 15%, with the ratio of horizontal to vertical displacements (rake) being almost identical. The maximum depth is ~ 20 km in the two cases.

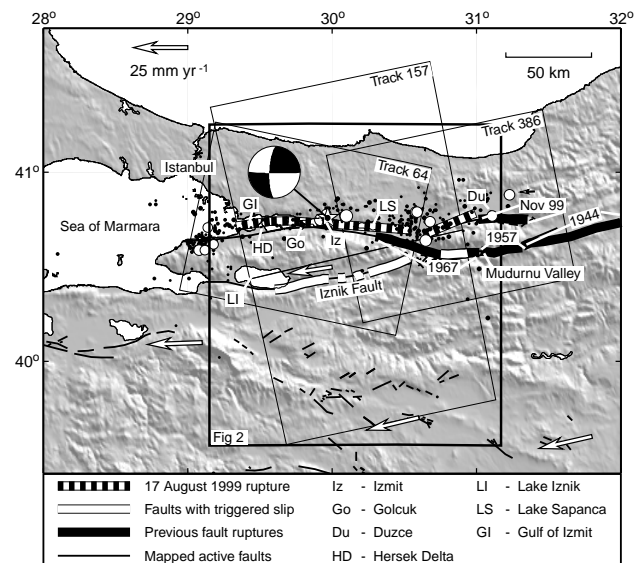


Figure 1. Topographic and tectonic map showing the extent of the 17 August 1999 Izmit earthquake rupture. Seismic activity (Kandilli Obs.) in the interval between our radar image acquisitions (13 August to 16 September) is shown as black dots with events larger than $M_d 4.5$ depicted by circles. The star indicates the epicentral location (Kandilli Obs.) with focal mechanism from the Harvard CMT solution. Arrows show the GPS-determined interseismic velocities relative to Eurasia [Reilinger *et al.*, 1997]. The inclined boxes delimit the coverage of our interferograms

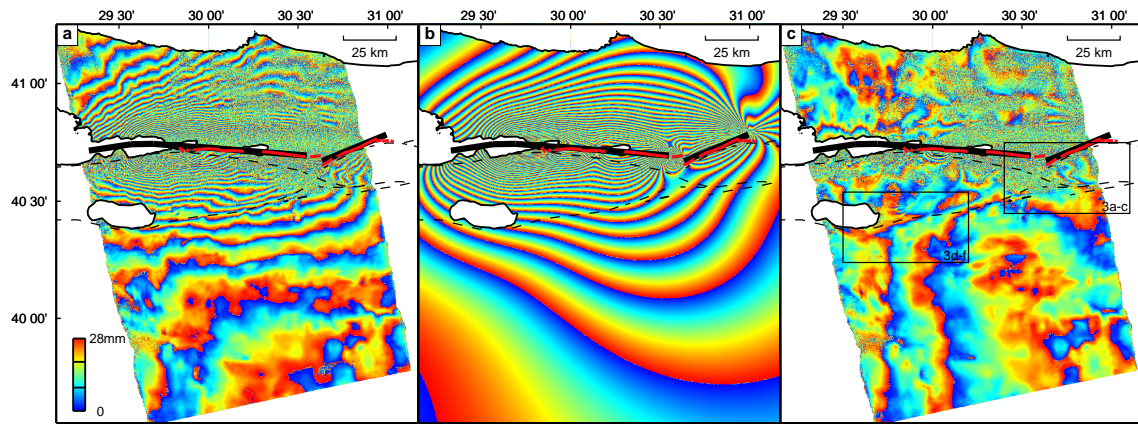


Figure 2. **a**, Radar interferogram for the Izmit earthquake (data copyright ESA) revealing the surface displacements, measured in the satellite's line-of-sight, in the 35-day period between the two image acquisitions (Table 1a). Each interference fringe is equivalent to 28 mm of displacement in the satellite line-of-sight, or approximately 70 mm if caused by pure horizontal motion. A correction for the small topographic contribution was made with a DEM constructed from ERS tandem interferograms and GTOPO30 data [Fielding *et al.*, 1999] and the interferogram was smoothed using a power spectrum filtering algorithm [Goldstein and Werner, 1998]. Red lines are the mapped surface rupture [Barka, 1999] and the dashed lines are previously mapped segments of the North Anatolian Fault [Şaroglu *et al.*, 1992]. **b**, Synthetic interferogram calculated using the elastic dislocation model described in the text that intersects the surface at the location shown by the thick black lines. **c**, Residual interferogram, obtained after subtracting **b** from **a**.

Our fault model (Table 2, Fig. 2) shows the western limit of rupture to be ~ 15 km west of the Hersek Delta, where over 1.5 m of slip is required to obtain a good fit to the interferograms. The rupture location passes just north of the delta, although the absence of data near the fault means we cannot be certain of this location to better than a few kilometres. Slip was a maximum of 4.5–5 m on the segment north of Golçuk and over 4 m between Izmit and Lake Sapanca, but is only 1.5–2 m where the rupture is 5–10 km north of segments that ruptured in 1967. The overall residual phase falls within the level of noise caused by atmospheric and

orbital error evident in the differences between the 35-day interferograms. An exception to this is in one region near Izmit where a large aftershock (13/9/99, M_d 5.8, Kandilli Obs.) occurred within the time span of the interferograms, contaminating the signal of the 17 August event.

Triggered Slip

By removing our model of coseismic deformation from the interferogram, we are able to detect small deformation signals associated with faulting away from the Izmit rupture.

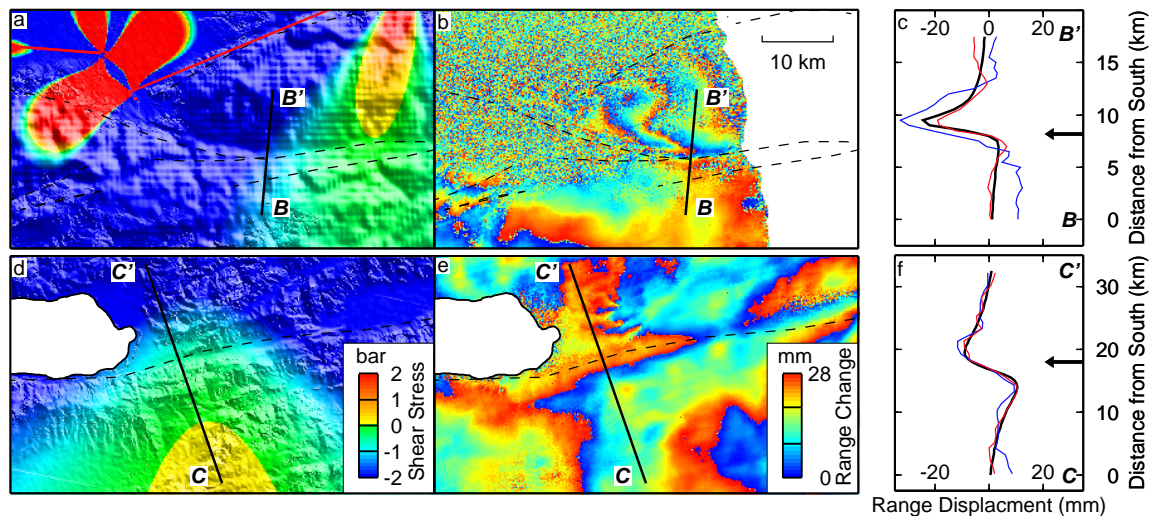


Figure 3. Evidence for triggered fault slip on Mudurnu Valley (**a-c**) and Iznik (**d-f**) faults. **a,d**, Static shear stress changes (vertical, E-W faults) calculated from our best-fitting elastic dislocation model of the Izmit earthquake, which intersects the surface at the red lines. Negative shear stress changes imply left-lateral shear, with shading from the DEM. Dashed lines are mapped segments of the North Anatolian Fault [Şaroglu *et al.*, 1992]. **b,e**, Residual interferogram (Fig. 2). The tight color gradients at the center of profiles B–B', C–C' coincide with the location of active faults. **c,f**, Range change profiles along B–B' (**c**), C–C' (**f**). Red line corresponds to the residual interferogram shown in **b,e** (ERS2 to ERS2, linear trend removed from **e**); Blue – residual of ERS1 interferogram; Black – range change calculated using an elastic dislocation model. The dislocation models shown assume pure horizontal (i.e. left-lateral) slip (Table 3).

Table 1. Details of ERS SAR data (©ESA).

ERS Track/Frame ^a	Date 1/2	Orbit 1/2 ^c	h_a ^c
a) 157/815,797(A)	13-8-99/17-9-99	22556(2)/23057(2)	1680
b) 157/815,797(A)	12-8-99/16-9-99	42229(1)/42730(1)	560
c) 64/2786(D)	20-3-99/15-10-99	20459(2)/43138(1)	1270
d) 386/810(A)	9-8-98/3-10-99	17274(2)/23286(2)	348

^a Ascending(A)/descending(D) pass; ^b Orbit numbers for ERS-1 (1) or ERS-2 (2); ^c Scene center altitude of ambiguity (metres).

Generally, the residual interferogram (Fig. 2) varies very smoothly. However, across the Mudurnu Valley and east of Lake Iznik, strong phase gradients remain in the residuals that are coincident with mapped active faults (Fig. 3). These signals are very similar in both 35-day interferograms, but could not be observed in the other datasets due to temporal decorrelation. Profiles of range change constructed across the Mudurnu Valley and Iznik faults (Fig. 3c,f) show that there is a range change decrease of 20–25 mm from south to north across both faults.

These apparent range changes are unlikely to be the result of atmospheric artefacts because of the spatial coincidence with active faults, and because atmospheric phase variations observed in the difference between the 35-day interferograms have longer wavelengths. Satellite geometry rules out topographic artefacts: topographic errors of over 4800m (ERS2) and 660m (ERS1) in the Mudurnu Valley, and 850m/300m on the Iznik strand, are required to generate 20 mm of range change.

We model the displacements on the Mudurnu Valley and Iznik faults using elastic models to determine best-fitting fault parameters. In both cases, continuity of the phase across the faults implies that slip was subsurface. InSAR detects only the component of displacement in the satellite line-of-sight, hence a variety of fault rakes can produce the observed range change. Solutions include pure left-lateral strike-slip, pure vertical (upthrown to north) and right-lateral with some vertical (Table 3), but the range changes could not have been caused by pure right-lateral slip. If the slip is left-lateral, its depth is shallow (0.6–1 km in Mudurnu Valley). Less slip is required for the purely vertical solutions, but over a larger depth range (0.6–3.5 km in Mudurnu Valley). Oblique right-lateral slip is also possible, provided that the vertical displacement causes a greater range change than

Table 3. Triggered slip fault parameters [0° rake = left-lat; 90° = vertical; 150,160° = oblique right-lat]

	Rake	Slip	Depth Range	M_0 (Nm)
Mudurnu Valley	0°	10cm	0.6–1 km	1.7×10^{16}
(Str. 280° , Dip 50° , Len. 10 km)	90°	1.9cm	0.6–3.5 km	2.4×10^{16}
	150°	7cm	0.6–15 km	4.5×10^{17}
Iznik Fault	0°	20cm	2.5–3.5 km	2.0×10^{17}
(Str. 260° , Dip 90° , Len. 30 km)	90°	1.4cm	2.5–12.5 km	1.4×10^{17}
	160°	8cm	2.5–20 km	1.4×10^{18}

the right-lateral slip. By varying the rake we find that, to produce the observed range change, rakes must be less than 165° and 155° at the Iznik and Mudurnu Valley respectively, and slip must extend over most of the seismogenic layer.

Our interferograms do not distinguish between slip occurring in aftershocks and aseismic triggered slip up to a month after the earthquake. However, earthquakes larger than $M_w \simeq 4.7-5$ would be required to cause sufficient deformation and there are no aftershocks, in these locations, that are sufficiently large (Fig. 1). In addition, the deformation has a ratio of fault slip to length of $\sim 5 \times 10^{-6}$ or less, an order of magnitude smaller than the typical ratio for seismic events [Pegler and Das, 1996]. This suggests that, unless this slip occurred preseismically or at the same time as the mainshock, it was the result of aseismic triggered slip.

Discussion and Conclusions

There are several explanations for triggered slip. Coseismic movement during the 17 August mainshock changed the static stress in the area [Parsons et al., 2000] by an amount that we can calculate using our slip model (Fig. 3a,d). At the locations of our profiles, left-lateral shear stress increases of 2.0 and 0.8 bars occurred on the Mudurnu Valley and Iznik faults. For these to create left-lateral slip, they would have to be larger than the right-lateral stresses accumulated interseismically. While this is possible for the Mudurnu Valley fault, which ruptured in 1967, it seems unlikely on the Iznik fault which has been seismically quiescent for the last 500 years [Ambraseys and Jackson, 2000]. However, it is possible that interseismic stress is released by continuous deformation in weak shallow layers. Any stress changes due to the Iznik event would then dominate and cause left-lateral slip.

Table 2. Source parameters of the Izmit Earthquake from InSAR. Where two parameter values appear, they are the result of separate inversions on interferograms *a,c,d* and *b,c,d* (Table 1). Other parameters are held fixed.

	Seismic ^a			Geodetic (6 segments, starting from West)			
Scarp Latitude	41.01° ^b	40.730°	40.744°	40.739°	40.726°	40.708°	40.728°
Scarp Longitude	29.97° ^b	29.450°	29.630°	29.812°	30.039°	30.347°	30.813°
Length / km	—	20.1	10.5	20.3	18.2	34.2	32.8
				Total Length = 136.1			
				Total $M_0 = 265,253$			
$M_0 / 10^{18}$ Nm ^c	288						
Slip ^d / m	—	1.7,1.6 (—) ^d	2.5,2.3 (—) ^d	4.9,4.7 (—)	4.6,4.4 (3-4) ^e	2.1,1.8 (0.5-4.5)	1.7,1.4 (1.5)
Strike	91°	$84,264^\circ$	$91,271^\circ$	$96,96^\circ$	$277,97^\circ$	$276,96^\circ$	$249,249^\circ$
Dip	87°	$88,84^\circ$	$86,88^\circ$	$86,87^\circ$	$88,88^\circ$	$81,85^\circ$	$61,81^\circ$
Rake	164°	$174,-174^\circ$	$171,-167^\circ$	$178,178^\circ$	$-178,177^\circ$	$-164,162^\circ$	$-168,-166^\circ$
d_{min} / km	17.0^b	0	0	0	0	0	0
d_{max} / km				20.0,21.6			

^aHarvard CMT solution; ^bCentroid Location; ^cAssuming Lamé elastic constants $\mu = 3.43 \times 10^{10}$ Pa, $\lambda = 3.22 \times 10^{10}$ Pa; ^dFigures in brackets refer to geological observations of surface slip [Barka, 1999]; ^eAn improved fit is obtained if slip is only 3.7m in the top 2 km

If the slip is predominantly right-lateral and occurs over most of the seismogenic layer thickness, then it cannot be caused by the change in static stress from the Izmit earthquake but instead is likely to be the result of release of tectonic stress accumulating in the North Anatolian Fault Zone due to the westward movement of central Turkey with respect to Eurasia (Fig. 1). These stresses can be released by transient dynamic unclamping due to the passage of seismic surface waves from the mainshock [Bodin *et al.*, 1994]. However, right-lateral slip requires the release of significantly more seismic moment (Table 3) than left-lateral or vertical slip solutions and, in the absence of other data, the smaller M_0 solutions are preferred.

Although triggered slip has been observed in only a limited number of cases [Sylvester, 1986; Bodin *et al.*, 1994; Price and Sandwell, 1998], it may well be a common occurrence. Most of the previous observations have been of small surface ruptures. In these examples, however, the interferometric fringes can be traced continuously across the faults showing that slip does not break the surface. Although the triggered slip is small compared to that in the main Izmit event, it is not a negligible part of the strain budget. For example, if slip is right-lateral with a magnitude of ~ 10 cm, it would represent ~ 10 years of strain accumulation, assuming a 2 cm/yr slip rate partitioned equally onto two faults. In future, it may be possible to use InSAR to determine displacements for triggered slip events using a number of different lines of sight, hence resolving the ambiguity in the slip mechanism.

Acknowledgments. This work is supported by NERC and the European Space Agency, and a NERC studentship, with Nigel Press Associates, to TJW. We thank Aykut Barka, Philip England, Kurt Feigl, Mark Haynes, Margaret Moore, Ross Stein, Roger Bilham and two anonymous reviewers for helpful discussions and comments; CNES and Kurt Feigl for support with the DIAPASON/PRISME software and Paul Rosen and Scott Hensley of JPL for the use of their ROLpac software.

References

- Ambraseys, N., Some characteristic features of the North Anatolian Fault Zone, *Tectonophysics*, *9*, 143–165, 1970.
- Ambraseys, N., and J. Jackson, Seismicity of the Sea of Marmara (Turkey) since 1500, *Geophys. J. Int.*, *In Press*, 2000.
- Barka, A., Slip distribution along the North Anatolian Fault associated with the larger earthquakes of the period 1939 to 1967, *Bull. Seismol. Soc. Am.*, *86*, 1,238–1,254, 1996.
- Barka, A., The 17 August 1999 Izmit earthquake, *Science*, *285*, 1858–1859, 1999.
- Bodin, P., R. Bilham, J. Behr, J. Gomberg, and K. Hudnut, Slip triggered on southern California faults by the 1992 Joshua Tree, Landers and Big Bear earthquakes, *Bull. Seismol. Soc. Am.*, *84*, 806–816, 1994.
- Bürgmann, R., P. Rosen, and E. Fielding, Synthetic aperture radar interferometry to measure Earth's surface topography and its deformation, *Ann. Rev. Earth. Planet. Sci.*, *28*, 169–209, 2000.
- Fielding, E., T. J. Wright, B. Parsons, P. England, P. Rosen, S. Hensley, and R. Bilham, Topography of northwest Turkey from SAR interferometry: Applications to the 1999 Izmit earthquake geomorphology and co-seismic strain (abstract), *Eos Trans. AGU*, *80*, 663, 1999.
- Goldstein, R. M., and C. L. Werner, Radar interferogram filtering for geophysical applications, *Geophys. Res. Lett.*, *25*, 4,035–4,038, 1998.
- Massonnet, D., and K. L. Feigl, Radar interferometry and its application to changes in the earth's surface, *Rev. Geophys.*, *36*(4), 441–500, 1998.
- Okada, Y., Surface deformation due to shear and tensile faults in a half-space, *Bull. Seismol. Soc. Am.*, *75*, 1,135–1,154, 1985.
- Parsons, T., S. Toda, R. Stein, A. Barka, and J. Dieterich, Heightened odds of large earthquakes near Istanbul: an interaction-based probability calculation, *Science*, *228*, 661–665, 2000.
- Pegler, G., and S. Das, Analysis of the relationship between seismic moment and fault length for large crustal strike-slip earthquakes between 1977–92, *Geophys. Res. Lett.*, *23*(9), 905–908, 1996.
- Price, E., and D. Sandwell, Small-scale deformations associated with the 1992 Landers, California earthquake mapped by synthetic aperture radar interferometry phase gradients, *J. Geophys. Res.*, *103*, 27,001–27,016, 1998.
- Reilinger, R., S. McClusky, M. Oral, R. King, M. Toksoz, A. Barka, I. Kinik, O. Lenk, and I. Sanli, Global Positioning System measurements of present-day crustal movements in the Arabia–Africa–Eurasia plate collision zone, *J. Geophys. Res.*, *102*, 9,983–9,999, 1997.
- Şaroglu, F., Ö. Emre, and İ. Kuşçu, *Active Fault Map of Turkey*, General Directorate of Mineral Research and Exploration (MTA), Eskişehir Yolu, 06520, Ankara, Turkey, 1992.
- Sylvester, A., Near-field tectonic geodesy, in *Active Tectonics (Studies in Geophysics Series)*, pp. 164–180, National Academy Press, Washington, D. C., 1986.
- Wright, T. J., B. Parsons, J. Jackson, M. Haynes, E. Fielding, P. England, and P. Clarke, Source parameters of the 1 October 1995 Dinar (Turkey) earthquake from SAR interferometry and seismic bodywave modelling, *Earth Planet. Sci. Lett.*, *172*, 23–37, 1999.

Barry Parsons, Tim Wright, Department of Earth Sciences, University of Oxford, Parks Road, Oxford, UK. (e-mail: barry@earth.ox.ac.uk; timw@earth.ox.ac.uk)

Eric Fielding, JetPropulsionLaboratory, 4800 Oak Grove Drive, Pasadena, CA, 91109, USA. (e-mail: ericf@sierras.jpl.nasa.gov)

(Received May 16, 2000; revised August 3, 2000; accepted September 25, 2000.)